Electron-Scattering Study of Nuclear Levels in Cobalt, Nickel, Lead, and Bismuth*

H. CRANNELL, R. HELM, H. KENDALL, J. OESER, AND M. YEARIAN
High-Energy Physics Laboratory, Stanford University, Stanford, California
(Received March 24, 1961)

We have observed inelastic scattering of 183-Mev electrons through angles of 40°–90° in the laboratory, leading to excitation of discrete nuclear excited states in Ni^{58}, Co^{59}, Ni^{60}, Pb^{208}, and Bi^{209}. The excitation energies were below 8 Mev. Born-approximation analysis of the measured inelastic form factors was used to deduce the multipolarities λ (when not previously known), and, by extrapolation, the transition rates for 15 corresponding gamma transitions. A number of groups of electric transitions for $\lambda=2$, 3, and 4 were observed, each group having strikingly similar form factors. In all but one of these groups the ratios G of the observed gamma transition rates to the single-particle predictions were greater than 15, and for some transitions from 30 to over 100. One of the groups, in cobalt and the nickels, contains the 1.33-Mev $E2$ transition to the first excited state of Ni^{60}. Another group consists of fast $E3$ transitions, seen in all five nuclei, from states known as the "anomalous levels." They included the transition to the first excited state in Pb^{208} ($G=31$) and a transition in Bi^{209} identical in energy and form factor. Among three slow $E4$ transitions in cobalt and the nickels was the 2.50-Mev $4^+\rightarrow 0^+$ transition in Ni^{60}. The $E4$, $E3$, and an $E2$ transition in Co^{59} identify states analogous to the 4^+, 3^-, and 2^+ seen in the neighboring even-even nuclei. The last two transitions are strongly enhanced. A pair of fast 4.30-Mev $E4$ transitions was observed in Pb^{208} and Bi^{209}; their speed ($G=37$) indicates they may constitute the lowest-energy configuration of 16-pole mode of excitation of the nuclear surface. Values of the collective vibrational parameters C_λ and B_λ and the degree to which some of the transitions exhaust ordinary sum rules support the conclusion that the inelastic scattering process is strongly exciting nuclear collective excitations. Some of the observed results are expected on the basis of the theory of collective vibrational excited states; some are the consequence of unidentified configurations.

I. INTRODUCTION

ELASTIC and inelastic scattering of high-energy electrons, in principle, provides a powerful tool for the investigation of nuclear structure, for not only is the electron-nucleus interaction known in great detail, but the large momentum transfers that can be effected by using primary electron energies above 100 Mev lead to cross sections that are very sensitive to the spatial structure of nuclear ground states or of nuclear excited states.[1] Large-angle scattering of high-energy electrons can easily induce nuclear transitions of high as well as low multipolarity, and provides one of the few means of studying nuclear resonance transitions with excitations greater than a few Mev accompanied by nuclear angular momentum changes larger than $3\hbar$. Theoretical understanding of elastic electron scattering is well advanced and more than adequate for the interpretation of present experiments[1,2]; quite fine structure in the charge distribution of the nuclear ground state can be distinguished by analysis of experimental cross sections. Inelastic electron scattering to discrete nuclear levels is, as yet, not as easily interpretable; a complete phase-shift analysis of the scattering process is much more complicated than for the elastic case and is not yet available. Born-approximation results have been published,[3] however, and, as in the elastic scattering case, are useful in interpreting experimental measurements. In the measurements reported here, inelastic scattering measurements have been made with nuclear excitations up to 7.5 Mev with a primary electron energy of 183 Mev. Similar transitions have been studied in two groups of nearly identical nuclei (Ni^{58}, Co^{59}, Ni^{60}; and Bi^{209}, Pb^{208}) in order to establish the similarity of different types of transitions in a manner as independent of analysis as possible. In addition, each transition form factor was compared with the Born-approximation predictions to establish the multipolarity and to determine, by extrapolation, the partial γ-ray decay rate to the ground state.

II. EXPERIMENTAL APPARATUS

Target materials in the form of metallic foils were placed at the focus of the momentum-analyzed electron beam of the Stanford linear accelerator. Electrons scattered by the target through angles from 40°–90° were momentum-analyzed with a 36-in. magnetic spectrometer. The detector was a 10-channel scintillation counter and Čerenkov counter telescope defining 10 adjacent momentum intervals in the image plane of the spectrometer. Each fractional momentum interval $\Delta p/p$ was equal to 0.0031, where Δp was the momentum acceptance defined by each counter element and p was the focused momentum. The primary beam was integrated after it passed through the target by either a Faraday cup or a secondary-emission monitor.[4] The apparatus has been described before, and the references contain additional information on the operation of the equipment.[1,5,6]

The relative efficiency of each of the 10 channels was determined at intervals of a few hours during the cross-

* This work was supported in part by the joint program of the Office of Naval Research, the U. S. Atomic Energy Commission, and the Air Force Office of Scientific Research.

[1] H. Crannell, R. Helm, H. Kendall, J. Oeser, and M. Yearian, Phys. Rev. **121**, 283 (1961).

[2] U. Meyer-Berkhout, K. W. Ford, and A. E. S. Green, Ann. Phys. **8**, 119 (1959).

[3] L. I. Schiff, Phys. Rev. **92**, 988 (1953), and **96**, 765 (1954); the latter paper is referred to as "LS" in the text. See also, J. H. Smith, Phys. Rev. **95**, 271 (1954).

[4] F. Bumiller and E. Dally, in *Proceedings of the International Conference on Instrumentation for High-Energy Physics, Berkeley, 1960* (to be published).

[5] J. I. Friedman, H. W. Kendall, and P. A. M. Gram, Phys. Rev. **120**, 992 (1960).

[6] H. W. Kendall, J. I. Friedman, E. F. Erickson, and P. A. M. Gram (to be published).

section measurements by counting at the flat part of the inelastic spectrum of electrons scattered from a C^{12} target. The number of counts detected by each channel was used to determine a correction factor applied to data measured by that channel. Normally, these efficiency factors were known to better than 3%, and they rarely deviated from a constant value beyond what was expected from statistical fluctuations in the number of observed events.

High momentum resolution was required to distinguish by energy loss the electrons that had scattered elastically or inelastically, leaving the nucleus in one or another discrete excited state. Contributions to the uncertainty in the determination of the residual nuclear excitation arose from the finite momentum spread of the primary electron beam, radiative and ionization processes occurring when the primary beam or scattered electrons passed through the target material or other foils or windows, aberrations in the focusing properties of the spectrometer, and the finite momentum acceptance of the elements of the electron detecting system described above. The fractional uncertainty in the primary electron beam momentum was normally adjusted to be in the range from 0.1%–0.2%. Electron bremsstrahlung and Landau straggling from target and foils and radiative processes occurring during the scattering process contributed an uncertainty in the values of the momenta of the scattered electrons of less than 0.2%. These effects could be calculated to high accuracy, and the measured momentum spectra of scattered electrons corrected for them. In practice, although bremsstrahlung and radiative corrections were applied to all the measured spectra, the correction program propagated uncertainties arising from statistical counting-rate fluctuations from each part of the measured spectra to all lower-momentum parts. (References 5 and 6 contain a more complete discussion of the correction progr um.) The effect was to reduce greatly the accuracy of inelastic cross-section determinations when their yields were much smaller than that from the elastic process at the same energy and angle. To reduce uncertainties from this source to a minimum, very thin target materials were used. Typical values for target thicknesses, measured in radiation lengths (r.l.), were 0.03 and 0.05 r.l. for Ni^{60} and Ni^{58}, and 0.03 r.l. for Pb^{208}.

Aberrations in the magnetic spectrometer made a negligible contribution to the observed momentum uncertainties. Theoretical studies[7] of the instrument used in the present series of experiments indicated the uncertainties introduced in the determination of a scattered-electron momentum p to be less than $10^{-3}p$, and this result was consistent with observed elastic peak widths. The fractional momentum resolution from all the effects discussed above was $\Delta p/p=0.45\%$ for the data reported here, and energies of discrete excited nuclear states in the present experiment could be determined to within an accuracy of 100–200 kev for strongly excited transitions.

III. DETERMINATION OF CROSS SECTIONS AND FORM FACTORS

Absolute cross sections for elastic and inelastic scattering were determined by comparison with electron scattering from the free protons in a polyethylene target.[8] The momentum spectra of electrons scattered from the polyethylene, the two Ni, the Co, the Bi, and the Pb targets were corrected for the varied efficiencies of the counters and normalized for a uniform integrated primary beam and number of target nuclei per cm^2 in the beam. Each spectrum was corrected for bremsstrahlung and radiative effects during scattering by using the momentum transfer in the scattering process and the total number of radiation lengths of material in the scattered electrons' path as parameters. The corrections

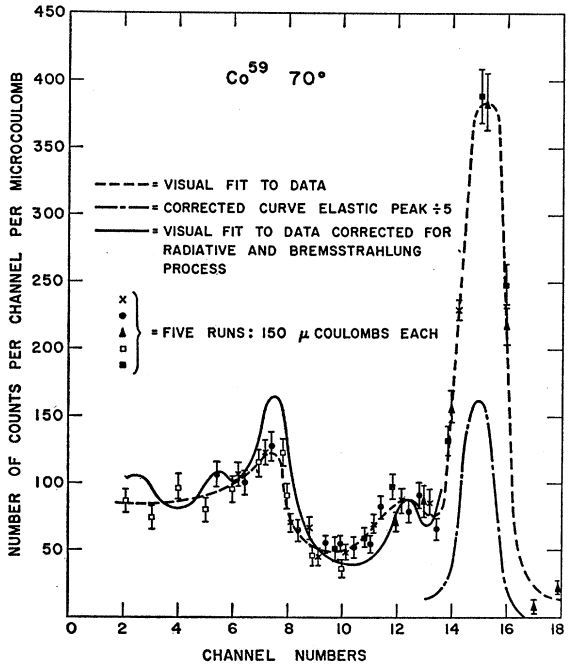

FIG. 1. In this figure and in Fig. 2 are shown the experimental data of a number of separate runs on the elastic and inelastic electron spectra from scattering of 183-Mev electrons from Co^{59} at $\theta=70°$ and Ni^{58} at $\theta=55°$, where θ is the laboratory scattering angle. The abscissas are scales determined from the momentum acceptance of the separate channels of the detector. Successive integers determine momentum intervals Δp such that $\Delta p/p=0.0031$. The deviation from a linear momentum scale is negligible over the ranges displayed. The zeros of the abscissas are arbitrarily chosen. The ordinates display the number of detected electrons per microcoulomb of integrated charge from the primary beam. They are proportional to $d^2\sigma/d\Omega dp$, the cross sections for the electron-scattering processes as observed with finite momentum resolution. The dashed curves are visual fits to the data, and the solid curves are the visual fits with bremsstrahlung and radiative corrections applied.

[7] D. L. Judd, Rev. Sci. Instr. **21**, 213 (1950); and F. Bumiller (private communication).

[8] F. Bumiller (private communication).

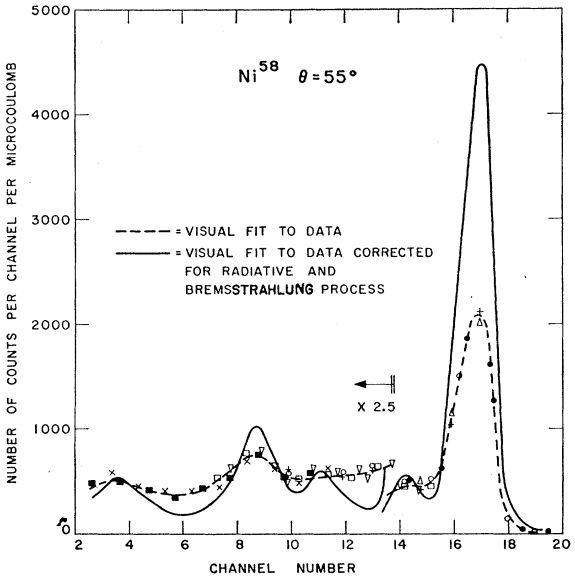

FIG. 2. Scattered-electron spectrum from a Ni^{58} target at $\theta=55°$. See caption to Fig. 1.

were applied using an IBM-610 computer and have been described in detail.[5,6] From these corrected spectra and the known electron-proton elastic scattering cross sections,[8] the unknown elastic and inelastic scattering cross sections could be determined. Figures 1 and 2 show some representative corrected and uncorrected scattered electron spectra. Usually 40–100 data points were taken covering the inelastic spectrum with 200–700 counts per point. At small scattering angles, the uncorrected spectra were dominated by the radiative tail of the large elastic scattering peak, and a number of the inelastic scattering peaks could be seen only with some difficulty. At about $\theta=55°$ to $\theta=60°$, where θ is the laboratory angle of scattering, the first diffraction dip in the elastic scattering cross section gave a more favorable ratio of inelastic to elastic scattering, and, as the cross sections were large, this was the region of most accurate inelastic scattering cross-section and nuclear excitation energy determinations. At larger angles (θ from 80°–90°), the ratio of inelastic to elastic yields was in general less favorable, the cross sections were much smaller than at the lower angles, and, as at the small-angle points, the accuracy of the measurements was somewhat reduced.

Elastic and inelastic scattering form factors are defined from the relation

$$\sigma_{\text{obs}}=\sigma_M\times|F|^2, \tag{1}$$

where, in Born approximation,[3]

$$|F|^2=\left|\int e^{iq\cdot r}\langle f|M|i\rangle d^3r\right|^2,$$

where $\langle f|M|i\rangle$ is the matrix element relevant to the transition; F is the form factor for a transition to a discrete nuclear state, either to the ground (elastic scattering) or to an excited nuclear state (inelastic scattering); σ_{obs} is the observed differential scattering cross section for primary energy E_0 and laboratory angle θ; and σ_M is the differential Mott scattering cross section for scattering from a spinless point nucleus with the same Z as the target material. Nuclear recoil effects were negligible from all targets except hydrogen in the present experiments, and corrections for them were neglected in the determinations of all cross sections. All of the inelastic F^2 distinguished in the present experiments and several representative elastic F^2 are plotted in Figs. 3–12. The inelastic F^2 are plotted against $qA^{\frac{1}{3}}$, where q is the four-momentum transferred to the nucleus in the elastic scattering. The four-momentum transfer is given to

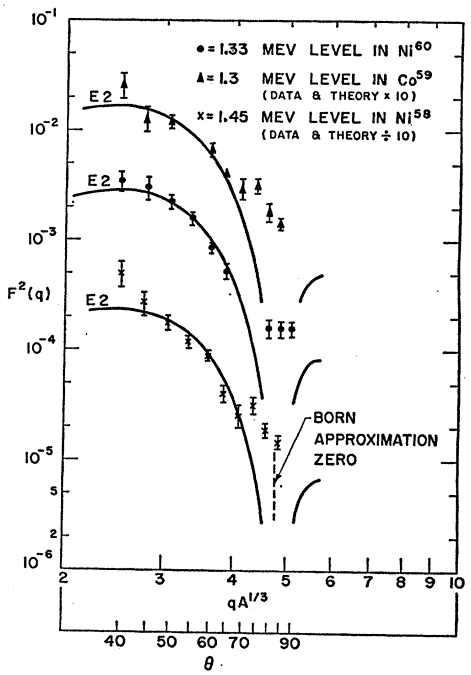

FIG. 3. In this and succeeding figures through Fig. 11 are shown the F^2 for the inelastic transitions observed in the present experiment. The abscissae are $qA^{\frac{1}{3}}$, where q is the momentum transfer in the scattering process and A is the target mass number. The errors shown are estimates of the errors arising from the determinations of the inelastic cross sections. The text contains a more complete discussion of these errors. The predicted F^2 for the various multipole assignments are shown as solid or dashed lines and are, unless otherwise noted, computed for $R_0=1.20$ f. The corrections arising from the change of the electron's wavelength when inside the nucleus have not been applied to these predictions. They have been applied to the transition rate measurements derived from these fits. The fitting parameters β_λ were the quantities determined by the comparisons of theory with experiment. The scales of laboratory angle θ are shown for $A=60$ and are approximately correct for $A=58$ and 59. The present figure shows F^2 for three similar $E2$ transitions in Ni^{58}, Co^{59}, and Ni^{60}. The breakdown of the Born approximation is evident in the region of the Born-approximation diffraction zero. In figures in which data and theory for more than one transition of similar character are shown, data and theory for the several sets are displaced by factors of ten for display purposes as noted in the figure legends.

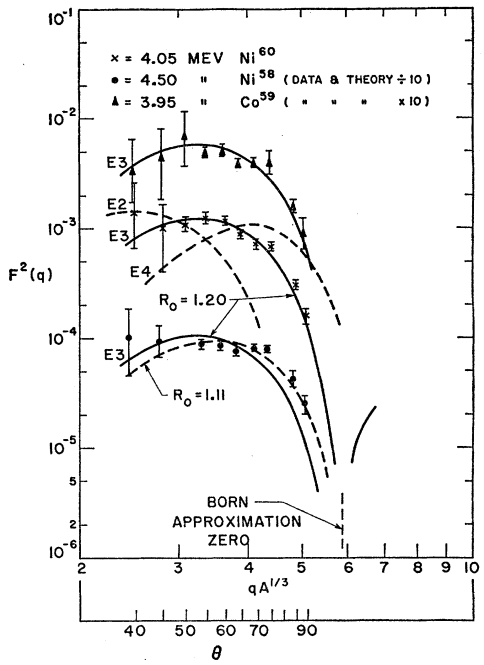

FIG. 4. Electric octupole transition F^2 in Ni^{58}, Co^{59}, and Ni^{60}. These are the "anomalous" transitions seen by Cohen and Rubin (reference 39). See caption to Fig. 3. A better fit to the Ni^{58} data is achieved by assuming $R_0=1.11$ f.

sufficient accuracy[9] by

$$q=2E_0\sin(\theta/2). \tag{2}$$

In Figs. 3–5, the laboratory angle θ, for $A=60$, is shown also. The F^2 are functions of q alone (or of $qA^{\frac{1}{3}}$) only in a first Born-approximation theory, and for inelastic magnetic nuclear transitions even this is not true. As we have identified only electric transitions and analyzed the data using the Schiff first Born-approximation theory,[3] this presentation is the most convenient (see Sec. IV).

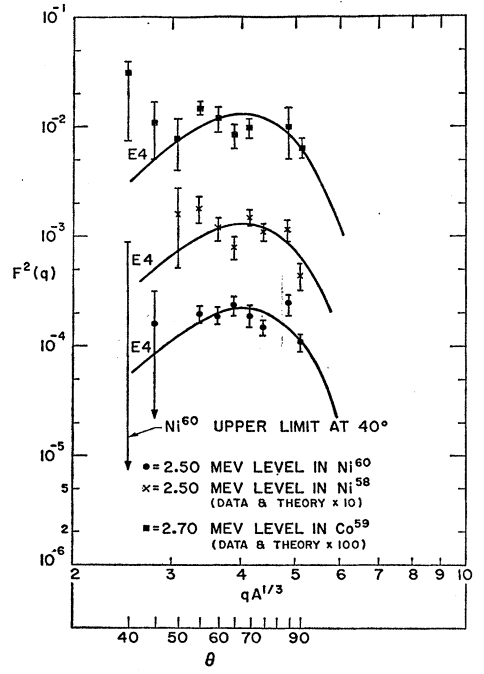

FIG. 5. Electric 16-pole transition F^2 in Ni^{58}, Co^{59}, and Ni^{60}. See caption to Fig. 3. The electron yields from Co^{59} were difficult to resolve from the background, and the small angle points may contain some contribution from background.

[9] R. Hofstadter, Ann. Rev. Nuclear Sci. **7**, 231 (1957).

IV. THEORETICAL INTERPRETATION OF THE DATA: ASSIGNMENT OF TRANSITION MULTIPOLES AND MEASUREMENT OF RADIATIVE WIDTHS

The analysis of the inelastic F^2 was based on the calculations of Schiff[3] and was similar to Helm's analysis of data from Sr^{88} and several d-shell nuclei.[10] The F^2, as defined by Eq. (1) for inelastic scattering involving a 2λ-pole transition between the nuclear ground state of spin I_g and an excited state of spin I_e, is given in Born approximation [Eq. (25) of LS,[3] whose notation we use] as

$$|F_\lambda(I_g,I_e)|^2=\frac{4\pi(2\lambda+1)}{2I_g+1}\times\sum_{m_g,m_e}\left|\int j_\lambda(qr)Y_{\lambda 0}\rho_\lambda(I_gm_g;\,I_em_e)d^3r\right|^2$$
$$=\beta_\lambda(I_gI_e)\left|4\pi\int j_\lambda(qr)\rho_\lambda{}^{g,e}(r)r^2dr\right|^2$$
$$=\beta_\lambda(I_gI_e)\,|f_\lambda{}^{g,e}|^2, \tag{3}$$

where

$$f_\lambda{}^{g,e}(q)=4\pi\int j_\lambda(qr)\rho_\lambda{}^{g,e}(r)r^2dr, \tag{4}$$

$\rho_\lambda(I_gm_g;\,I_em_e)$ is the matrix element for the transition; and we have assumed that the ρ_λ have the same radial dependence, allowing the factorization of the radial integral. Equation (3) gives the square of the transition form factor associated with the transition charge matrix element ρ_λ. The expressions (3) and (4) constitute the leading term in the cross section for electric transitions

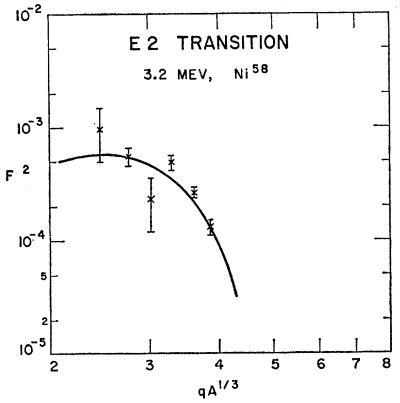

FIG. 6. 3.2-Mev $E2$ transition F^2 in Ni^{58}. See caption to Fig. 3.

[10] R. Helm, Phys. Rev. **104**, 1466 (1956); and Stanford University Ph.D. thesis, 1956 (unpublished).

of multipole order λ. We have neglected contributions from the transition magnetization and transition current matrix elements to the total transition rate for electric transitions, in accordance with the estimates of Schiff.[3] The same estimates allow a neglect of the entire class of magnetic transitions, justified *a posteriori* by the fact that all the $|F|^2$ seen in the present experiment can be fitted by assuming electric 2λ-pole for some choice of λ. The quantity $\beta_\lambda(I_g,I_e)$ includes the terms of the nuclear-orientation summations. It depends strongly on the nuclear model.

An approximate form for the F^2 of Eq. (3), for small q, can be found by expanding the spherical Bessel function and retaining the leading term:

$$\lim_{q\to 0}|F_\lambda(I_g,I_e)|^2\cong\beta_\lambda(I_g,I_e)q^{2\lambda}\left[\frac{\langle r^\lambda\rangle_{g,e}}{(2\lambda+1)!!}\right]^2, \quad (5)$$

where

$$\langle r^\lambda\rangle_{g,e}=4\pi\int {}^\lambda\rho_\lambda{}^{g,e}(r)r^2dr, \quad (6)$$

and $(2\lambda+1)!!\equiv(2\lambda+1)\times(2\lambda-1)\times\cdots\times3\times1$. Equation (5) can be combined with an expression for the partial gamma decay rate from the excited to the ground state derived by Ravenhall,[11] giving

$$\Gamma_\lambda(I_e\to I_g)=\frac{2I_g+1}{2I_e+1}\frac{\beta_\lambda(I_g,I_e)}{[(2\lambda+1)!!]^2}\times\frac{4Z^2\kappa^{2\lambda}r_{g,e}{}^{2\lambda}}{137}\frac{\lambda+1}{2\lambda}\left(\frac{\epsilon}{E_0}\right)^{2\lambda}\frac{\epsilon}{\hbar}, \quad (7)$$

where $\kappa=E_0/\hbar c$, and ϵ is the nuclear transition energy. It should be noted that Eqs. (3)–(7) are not valid for $\lambda=0$. The relations replacing these equations are discussed in reference 10.

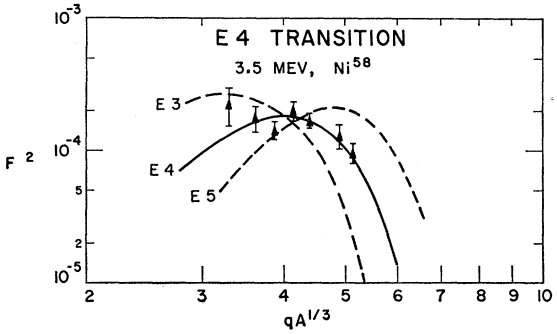

FIG. 7. 3.5-Mev $E4$ transition F^2 in Ni^{58}. See caption to Fig. 3.

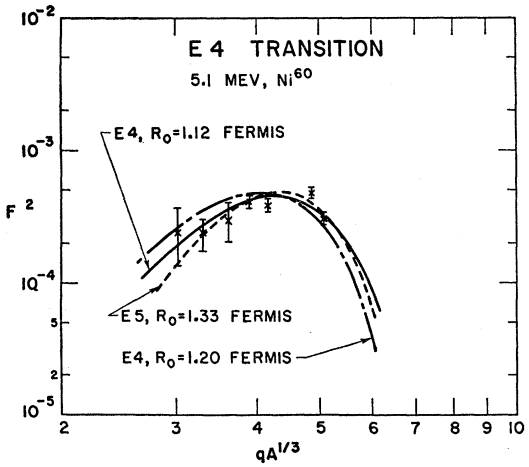

FIG. 8. 5.1-Mev electric 16-pole transition F^2 in Ni^{60}. See caption to Fig. 3. The fit to the data can be improved by using $R_0=1.12$ f. The prediction from an $E5$ multipole assignment is shown, also. The large value of R_0 probably excludes this assignment.

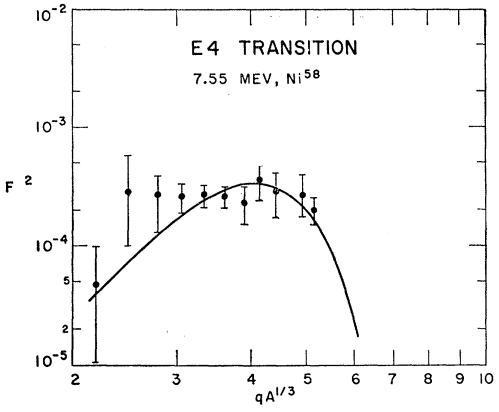

FIG. 9. 7.55-Mev electric 16-pole transition F^2 in Ni^{58}. See caption to Fig. 3.

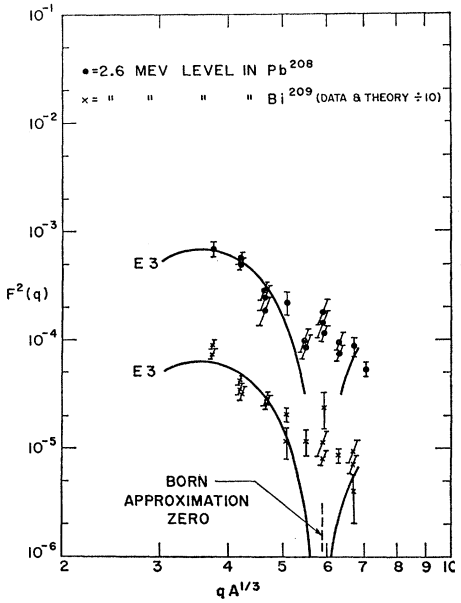

FIG. 10. 2.6-Mev $E3$ transition F^2 for Pb^{208} and Bi^{209}. These are the "anomalous" transitions similar to those shown in Fig. 4. The 2.6-Mev level in Pb^{208} is the first excited state. See caption to Fig. 3.

[11] D. G. Ravenhall (private communication, referred to in reference 10).

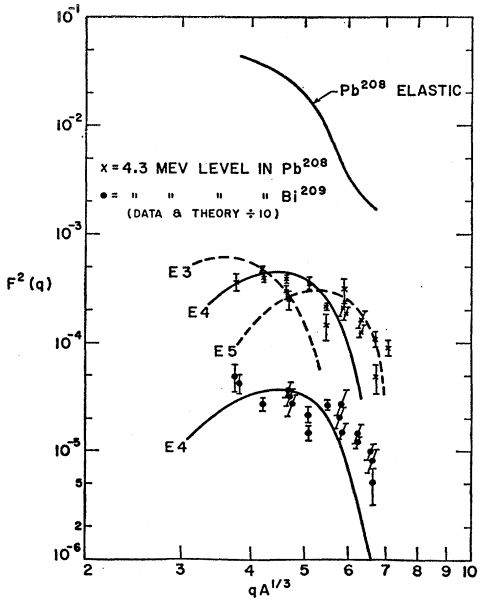

FIG. 11. 4.3-Mev electric 16-pole transition F^2 in Pb^{208} and Bi^{209}. Predictions from $E3$ and $E5$ multipole assignments are also shown. See caption to Fig. 3. The elastic F^2 for scattering from Bi^{209} is shown for comparison. These elastic data have been analyzed by Crannell *et al.* (reference 1).

cussed by Schiff[3]; they are not relevant to the analysis of these measurements.

Following the work of Helm,[10] we make a very simple assumption concerning the form of M of Eq. (1) for the cases of interest wherein $\lambda>0$ and we desire inelastic form factors. We assume that

$$M=\rho(\mathbf{r})=\int\rho_0(\mathbf{r}'-\mathbf{r})\rho_1(\mathbf{r}')d^3r', \tag{8}$$

where

$$\rho_0(\mathbf{r})=\delta(\mathbf{r}-\mathbf{R}),$$
$$\rho_1(\mathbf{r})=(2\pi g^2)^{-\frac{3}{2}}\exp(-r^2/2g^2),$$

and

$$\int\rho_1(\mathbf{r})d^3r=1.$$

The use of a folded charge distribution in a Born-approximation form factor of the form of Eq. (1) allows it to be factored into the products of the form factors for ρ_0 and ρ_1 separately. The square of the form factor associated with ρ_1 may be factored from Eq. (1). Then, $\rho_0(\mathbf{r})$ is the delta-function approximation suggested as an approximation for $\rho_\lambda(\mathbf{r})$ by LS.[3] The transition charge matrix element is thus described by a smeared delta function using the Gaussian function $\rho_1(\mathbf{r})$, with smearing parameter g. These assumptions are similar to the use of the spatial derivative of the static nuclear charge distribution as the distribution of the nuclear time-varying field. For these choices of ρ_0 and ρ_1, Eq. (3) takes the form

$$|F_\lambda(I_g,I_e)|^2=\beta_\lambda(I_g,I_e)\left|4\pi\int j_\lambda(qr)\rho_0(r)r^2dr\right|^2|F_\lambda(q)|^2$$
$$=\beta_\lambda(I_g,I_e)[j_\lambda(qR)]^2\exp(-q^2g^2), \tag{9}$$

where we have used

$$F_\lambda(q)=(2\pi g^2)^{-\frac{3}{2}}\int\exp(-r^2/2g^2)e^{-i\mathbf{q}\cdot\mathbf{r}}d^3r=\exp(-q^2g^2/2).$$

Equation (9) then determines the q dependence of the inelastic $|F|^2$ provided accurate assignments of R and g are made. We have made these assignments using the values of R and g determined from the elastic scattering data of Helm[10]: R is assumed to have the form $1.20\times A^{\frac{1}{3}}$ fermi and $g=0.95$ fermi. As used here, R is the radius of the equivalent uniform charge distribution and has been determined by Born-approximation analysis of elastic electron scattering. These charge distributions are in agreement with those found by the accurate phase-shift analysis of the relative elastic-scattering cross sections of Hahn *et al.*[12] and the more recent absolute cross sections of Crannell *et al.*[1] Within the present theory, with the assumptions concerning R and g, the measured inelastic $|F|^2$ determine only $\beta_\lambda(I_g,I_e)$ and λ (for those cases for which it was not previously known). In particular, the positions of the diffraction zeros predicted by the form of Eq. (9) are not subject to adjust-

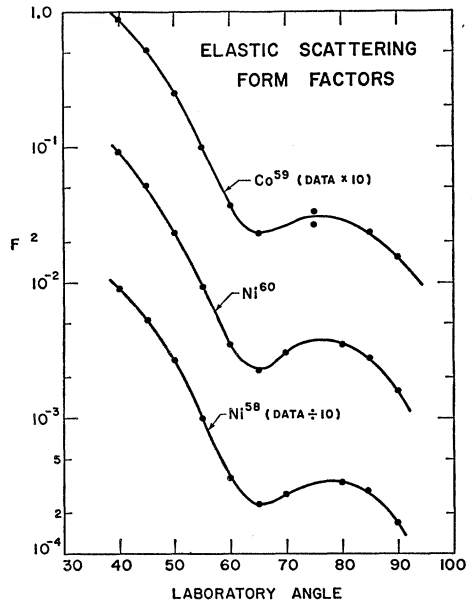

FIG. 12. Elastic F^2 for Ni^{58}, Co^{59}, and Ni^{60}. The errors are standard deviations arising from counting statistics and are about as large as the data points. The curves are visual fits to the data. The abscissa is the laboratory angle of scattering. These and other elastic data from Co^{59} have been analyzed by Crannell *et al.* (reference 1).

[12] B. Hahn, D. G. Ravenhall, and R. Hofstadter, Phys. Rev. **101**, 1131 (1956).

ment. The experimentally determined values of $\beta_\lambda(I_g,I_e)$ can be used in Eq. (7) to find the measured partial decay rates $\Gamma_\lambda(I_g \rightarrow I_e)$ for the gamma transitions. The values of $\Gamma_\lambda(I_e \rightarrow I_g)/\Gamma_{sp}(\lambda, I_e \rightarrow I_g)$ can then be computed from Γ_{sp}, the Weisskopf single-particle estimates as given by Mozskowski.[13] In evaluating the Γ_{sp}, we have used, for r, the nuclear radius $r=R_0A^{\frac{1}{3}}$, where R_0 was taken to be 1.20 f. The expression $\Gamma_\lambda/\Gamma_{sp}$ is the same for electric multipoles as $B_{obs}(E\lambda)/B_{sp}(E\lambda)$; where $B(E\lambda)$, the reduced transition probability, is defined by Alder *et al.*[14]; $B_{obs}(E\lambda)$ is the observed value; and $B_{sp}(E\lambda)$ is the Weisskopf single-particle estimate. We will use G for the ratio $\Gamma_\lambda/\Gamma_{sp}$.

V. EXPERIMENTAL RESULTS

The comparison of the predictions of Eq. (9) with the experimental data is shown in Figs. 4–10. The breakdown of the Born approximation is evident in every case in which the data span the value of q at the Born-approximation zero. A number of the multipolarities of the nuclear transitions, observed in these scattering experiments, are known from radioactive-decay scheme studies or from nuclear-reaction data.[15] In Ni^{60} the 1.33-Mev level is known to be 2^+, as is the 1.45-Mev level in Ni^{58}. The 2.60-Mev level in Pb^{208} is 3^- and the transition E3. The 2.50-Mev level in Ni^{60} has spin 4 and even parity; the transition is $E4$. Satisfactory fits to the electron-scattering data for all of these transitions have been made using these assignments to select the appropriate form of Eq. (9). On the basis of the near identity of the measured form factor of the 1.30-Mev transition in Co^{59} to both the 1.33-Mev transition in Ni^{60} and the 1.45-Mev transition in Ni^{58}, we have concluded that it, too, is $E2$. The spin assignment for this level is not determined unambiguously, however; it could well be the $\frac{3}{2}^-$ level seen by Mazari *et al.*[16] at 1.2 Mev. We regard the multipolarity assignment for this transition made from the present data as unambiguous. From comparisons with other transitions of comparable energy and known multipolarity, unambiguous $E3$ assignments are made for the 3.95-Mev transition in Co^{59} and the 2.60-Mev transition in Bi^{209}. In Fig. 4 are shown predictions for $E2$ and $E4$ assignments for the known 4.50-Mev $E3$ transition in Ni^{60}; they are clearly excluded by the data. In the same figure, the effect of a small alteration in R is shown in the prediction for the $E3$ form factor of the 4.50-Mev level in Ni^{58}. The spin assignments for all the excited states in odd-A nuclei, seen in the present experiment, are not determined uniquely by the data. It is possible that more than one level contributes to our observed yields. This point is discussed further in Sec. VI.

No other experimental data are available to select the multipolarity of the remaining transitions whose $|F|^2$ were measured here. Multipolarity assignments were made on the basis of the best fits using the theoretical predictions of different λ. The 4.30-Mev transitions in Bi^{209} and Pb^{208} were found to be the same, within experimental error, and did not fit the predictions for $E3$ transitions, contrary to the preliminary analysis reported earlier.[17] Figure 8 shows attempted fits for $E3$, $E4$, and $E5$ multipolarities to the data on the 5.1-Mev transition in Ni^{60}. The data suggest an $E4$ argument: The fit is about as satisfactory as the theoretical fit to the data of the known 2.50-Mev $E4$ transition in the same nucleus. Uncertainties in the determination of the radius parameter R and the surface thickness parameter g are great enough that $E3$ or $E5$ assignments are probably not excluded, although a fit to an $E5$ prediction requires $R_0=1.33$ fermi, a large value. The character of the 3.50-Mev level in Ni^{58} is poorly determined by the amount of data available; the data suggest an $E4$ assignment. Very little empirical or theoretical information exists that would allow estimates of the ambiguity in the multipolarity assignments.

The values of $\beta_\lambda(I_g,I_e)$, determined from the fitting procedures discussed above, were used with Eq. (7) to find the partial γ-ray transition rates for the excited-state to ground-state γ ray. These values are listed in Table I. The transition rates are listed in Table II. The value of $\kappa^{2\lambda}\langle r^\lambda\rangle_{g,e}^2$ in Eq. (7) has been taken to be $(\kappa R)^{2\lambda}$ multiplied by a factor to correct for the change of wavelength of incident electron when inside the nucleus. This correction factor is $[1+(3Z\alpha/2\kappa R)]^{-2\lambda}$, where α is the fine-structure constant. The factor varied from 0.764 for an $E2$ transition for $Z=28$ to 0.279 for an $E5$ transition for $Z=82$. This factor was not applied in the development of Eq. (9) as the value of R used was determined from uncorrected elastic Born-approximation data.[10]

For levels that constitute the first excited nuclear state, the γ-decay rates are the total rates; for transitions from the 4.05-Mev level in Ni^{60} and from the 4.5-Mev level in Ni^{58}, the ratios of the intensities of ground-state gamma branch to the $E1$ stopover transitions ending in the first excited 2^+ states were measured by Crut and Wall.[18] From these data, we have calculated the gamma transition rates for these $E1$ transitions. They are enormously attenuated, the values of G being about 3×10^{-6}, with errors estimated to be greater than 50%. The γ-ray branching ratio between the 1.17-Mev γ ray and the 2.50-Mev γ ray from the 2.50-Mev 4^+ level in Ni^{60} has been measured by Morinaga

[13] S. Mozskowski, in *Beta- and Gamma-Ray Spectroscopy*, edited by Kai Siegbahn (Interscience Publishers, Inc., New York, 1955), p. 390.

[14] K. Alder, A. Bohr, T. Huus, B. Mottelson, and A. Winther, Revs. Modern Phys. 28, 432 (1956).

[15] Data on the decay schemes are taken principally from *Nuclear Data Sheets*, National Academy of Sciences—National Research Council (U. S. Government Printing Office, Washington, D. C., 1959).

[16] M. Mazari, A. Sperduto, and W. W. Buechner, Phys. Rev. **107**, 365 (1957).

[17] H. Crannell, R. Helm, H. Kendall, J. Oeser, and M. Yearian, Bull. Am. Phys. Soc. 5, 270 (1960).

[18] N. S. Wall (private communication). We appreciate permission to use these unpublished data.

TABLE I. Values of β_λ, the fitting parameters of the Born-approximation inelastic form factors for transitions of angular momentum change λ, as defined by Eq. (9) of the text. The nuclear radius R was taken to be $R_0A^{\frac{1}{3}}$ for $R_0=1.20$ f unless otherwise noted. The errors are estimates from the fitting procedure in which disagreement near the region of the Born-approximation zeros was neglected. In these regions the Born approximation is known to be inadequate. The "anomalous" transitions are those enhanced $E3$ seen by Cohen and others in inelastic proton scattering (reference 39). The uncertainties in the transition energies are between 0.1 and 0.2 Mev.

Nuclide	ϵ (Mev)	λ	R_0 (f)	$\beta_\lambda\times10^2$	Remarks
Ni^{58}	1.45	2	1.20	4.5 ±1.20	
	3.20	2	1.20	1.1 ±0.4	
	4.50	3	1.11	4.3 ±0.6	Better fit
			1.20	4.7 ±1.2	Anomalous
	3.51	4	1.20	2.2 ±0.5	
	7.55	4	1.20	4.0 ±1.0	
	2.50	4	1.20	1.50±0.45	
Co^{59}	1.3	2	1.20	3.1 ±0.4	
	3.95	3	1.20	2.6 ±0.5	Anomalous
	2.7	4	1.20	1.2 ±0.5	
Ni^{60}	1.33	2	1.20	5.4 ±0.6	
	4.05	3	1.20	5.7 ±0.9	Anomalous
	2.50	4	1.20	2.7 ±0.5	
	5.1	4	1.1	5.0 ±0.8	Parameters for best fit
			1.2	5.4 ±0.8	
		5	1.33	12.5 ±1.4	Parameters of $E5$ fit
Pb^{208}	2.60	3	1.20	1.7 ±0.4	
	4.3	4	1.20	1.9 ±0.6	
Bi^{209}	2.60	3	1.20	1.6 ±0.5	
	4.30	4	1.20	1.7 ±0.6	

and Takahashi[19]; from this information, the partial decay rate for the 1.17-Mev $4^+\rightarrow2^+$ transition between the 2.50-Mev and the 1.33-Mev levels was derived. The branching ratio for γ-ray emission from the 2.50-Mev level in this nucleus to the second 2^+ state at 2.18 Mev must be very weak; it has not yet been observed.[15] The branching ratio of the intensity of the 190-kev γ ray to the 1.29-Mev ray leading to the ground state of Co^{59} is known.[15] Assuming the electron excitation is populating this state, the partial transition rate for the 190-kev line can be determined. The assumption may not be a good one; the point is discussed in Sec. VI.

There were a number of sources of error in the measurements of the form factors beyond those one would expect from the errors arising from counting-rate statistical fluctuations. There was, occasionally, a substantial background to be subtracted from observed peaks in addition to those subtracted during the radiative correction program. The scattered-electron momentum resolution of the equipment was not sufficient to resolve, clearly, the higher-energy nuclear transitions, and in more than one spectrum evidence is seen for the presence of unresolved transitions. For example, in Co^{59} there are more than 40 known nuclear levels in the range from 1.097-Mev to 3.95-Mev excitation. The present experiment distinguishes only three of these levels clearly; but others with inelastic cross sections, less than 10% of the transitions of low intensity observed here, could not be excluded from the spectra. There was a low background in the Co^{59} spectra that can be attributed to excitation of many of these levels. This background could not be resolved into transitions to discrete states. Small fluctuations in the operation of the electronic equipment, or in the stability of the magnetic spectrometer, contributed little error to elastic cross-section measurements but constituted a serious source of error in measuring the smaller inelastic cross sections because of the propagation of errors in the radiative correction program. The errors in the $|F|^2$ shown in Figs. 3–12 are standard deviations, estimated from the standard deviations of the number of counts in the inelastic peaks of the uncorrected scattered electron spectra and from the standard deviations of the estimated background subtraction. No quantitative calculation of the propagation of errors through the correction program was attempted, and the errors indicated on the plotted data points should be considered as lower bounds. The lower-angle points, in particular, required large bremsstrahlung subtractions and were more subject to undetected errors.

The errors ascribed to the determination of the gamma transition rates are only from fitting the assumed F^2 curves to the data, and do not include estimates of error in the Born-approximation theory, in the simplified assumptions concerning the transition charge densities, or in the choice of R and g. It is interesting to note that, in the few cases in which comparison is possible with measurements by other techniques, the results rarely disagree beyond what would be expected from the stated errors in the measurements. Table III contains all known comparisons of measurements of γ-ray transition rates by electron scattering from medium- and high-Z nuclei with determinations by other techniques. A few comparisons are shown for transitions for which the Born approximation should be adequate. These comparisons provide what are perhaps the best estimates of the reliability of electron-scattering measurements in determining these rates, just as the comparisons of Born-approximation and phase-shift calculations of elastic scattering provide the best estimates of the validity of the approximate cross sections. The nominal criterion for validity of Born approximation is $Z\alpha\ll1$. For the nickel-cobalt group $Z\alpha=0.24$, and for lead and bismuth it is ~0.6. The agreements between theory and experiment, as shown in Table III, are surprisingly good, although the number of known comparisons for $Z\gtrsim12$ is limited. The older electron-scattering results shown in this table were made on the basis of poorly defined absolute cross sections[10]; that contributed an error to those measurements that has no analog in the results of the present measurements. The electron-scattering technique appears to overestimate the transition rates when compared with the results of other measurements; but,

[19] H. Morinaga and K. Takahashi, J. Phys. Soc. Japan 14, 1460 (1959).

TABLE II. The measured γ-ray transition rates Γ_m given here for transitions ending in the ground state were deduced from the inelastic electron scattering results (given in Table I) using the extrapolation results of Ravenhall, Eq. (7). Γ_{sp} is the single-particle estimate of the gamma transition rate using the equations of reference 13 and nuclear radii $R=R_0A^{\frac{1}{3}}$ for $R_0=1.20$ f. The rates for four transitions between excited states were found using γ-ray branching ratios taken from other work. The $M1$ transition rate for the 0.191-Mev ray in Co^{59} requires the assumption that the electron scattering populates the 1.29 level (see references 15 and 16), an assumption that may be incorrect. The values of Γ_m for the $E1$ transitions in the nickel isotopes depend on unpublished measurements of Crut and Wall.[18] The $E1$ assignment is taken from their measured α, γ angular distributions (reference 37). Small admixtures of $M2$ or $E3$ are not excluded by their data. The value of Γ_m for the 1.17-Mev $E2$ transition in Ni^{60} depends on a measurement by Morinaga and Takahashi.[19] The assumptions concerning the spins of the states excited in the odd-A nuclei are important in determining the values of Γ_m through the statistical factors. Other evidence, discussed in the text, suggests that these transitions may be to groups of closely spaced states. For such cases, the values of β_λ given in Table I are a better guide to the collective properties of the excited states than the values of $G=\Gamma_m/\Gamma_{sp}$ given here. The errors given are consequent on the errors in the determination of the β_λ and do not include errors introduced by the Born approximation or the approximations to the nuclear transition matrix elements. Other evidence, discussed in Sec. IV, indicates that our techniques may overestimate Γ_m by an amount which may be as great as a factor of two. See also Table III.

Multipolarity	Nuclide	ϵ (Mev)	Γ_m (sec^{-1})	Γ_{sp} (sec^{-1})	$G=\Gamma_m/\Gamma_{sp}$	Remarks
$M1$	Co^{59}	0.191	$(4.88\pm0.63)\times10^{11}$	1.99×10^{11}	2.45 ± 0.31	$\frac{3}{2}^-\rightarrow\frac{5}{2}^-$ transition between excited states from 1.3-Mev level
$E1$	Ni^{58}	3.05	$(3.3\pm1.7)\times10^{11}$	...	...	From 3^- level (4.50 Mev) to 2^+ level (1.45 Mev)
	Ni^{60}	2.72	$(1.64\pm0.8)\times10^{11}$	5.2×10^{16}	$(3.2\pm1.6)\times10^{-6}$	From 3^- level (4.05 Mev) to 2^+ level (1.33 Mev)
$E2$	Co^{59}	1.30	$(7.4\pm0.95)\times10^{12}$	1.66×10^{11}	44 ± 5.7	
	Ni^{58}	1.45	$(1.56\pm0.2)\times10^{12}$	1.09×10^{11}	14.3 ± 1.9	
	Ni^{60}	1.33	$(1.27\pm0.15)\times10^{12}$	7.45×10^{10}	17.1 ± 2.1	
	Ni^{58}	3.2	$(2.58\pm0.94)\times10^{13}$	5.78×10^{12}	4.45 ± 1.6	
	Ni^{60}	1.17	$(3.25\pm0.6)\times10^{10}$	3.78×10^{10}	0.885 ± 0.17	From 4^+ level (2.50 Mev) to 2^+ level (1.33 Mev)
$E3$	Co^{59}	3.95	$(5.0\pm0.96)\times10^{10}$	3.1×10^{9}	16.5 ± 3.1	Assuming $I_e=13/2$
			$(3.52\pm0.67)\times10^{11}$	7.5×10^{9}	47.0 ± 9	Assuming $I_e=\frac{1}{2}$
	Ni^{58}	4.50	$(5.95\pm0.83)\times10^{10}$	4.53×10^{9}	13.2 ± 1.8	
	Ni^{60}	4.05	$(3.64\pm0.58)\times10^{10}$	2.29×10^{9}	15.9 ± 2.5	
	Ni^{60}	5.1	$(7.78\pm2.0)\times10^{10}$	1.0×10^{10}	7.8 ± 2.0	$E4$ is a better multipole assignment
	Pb^{208}	2.6	$(3.80\pm1.4)\times10^{10}$	1.23×10^{9}	30.8 ± 11.4	
	Bi^{209}	2.6	$(1.5\pm0.47)\times10^{11}$	2.79×10^{10}	54.2 ± 17	Assume $I_e=15/2$
			$(6.0\pm1.9)\times10^{11}$	5.43×10^{9}	110.0 ± 34	Assume $I_e=\frac{3}{2}$
$E4$	Co^{59}	2.70	$(1.1\pm0.46)\times10^{5}$	7.64×10^{3}	14.0 ± 5.9	Assume $I_e=15/2$
	Ni^{58}	2.50	$(0.7\pm0.21)\times10^{4}$	3.20×10^{3}	2.2 ± 0.66	
	Ni^{58}	3.51	$(2.92\pm0.66)\times10^{5}$	1.17×10^{4}	2.50 ± 0.57	Best multipole assignment
	Ni^{60}	2.50	$(1.3\pm0.24)\times10^{4}$	3.61×10^{4}	3.62 ± 0.67	
	Ni^{60}	5.1	$(1.58\pm0.24)\times10^{7}$	3.2×10^{6}	4.9 ± 0.73	Best multipole assignment
	Pb^{208}	4.3	$(2.23\pm0.7)\times10^{8}$	6.28×10^{6}	36.6 ± 12	
	Bi^{209}	4.3	$(9.74\pm3.4)\times10^{8}$	3.54×10^{7}	27.4 ± 9.6	Assume $I_e=17/2$
			$(8.75\pm3.1)\times10^{9}$	3.25×10^{7}	269.0 ± 95	Assume $I_e=\frac{1}{2}$
$E5$	Ni^{60}	5.1	$(4.66\pm1.5)\times10^{8}$	171	27.2 ± 8.7	$E4$ is a better multipole assignment

in general, it is not by as much as a factor of two. It is likely that the neglect of the current and magnetization terms in developing Eq. (9) is responsible for some overestimation; the neglect would contribute an error in this direction.

VI. DISCUSSION OF RESULTS

A. Introduction

A number of descriptions have been given of the systematic appearance of 2^+ first excited states in even-even nuclei which do not have a large permanent ground-state deformation.[14,20,21] These excited states are interpreted as consisting of vibrational oscillation of the nuclear surface about a near spherical equilibrium shape; the excitation energy corresponding to the energy of one phonon. The simple phonon model predicts strongly enhanced $E2$ transitions from the first excited state to the ground state, an enhancement observed experimentally, and, for two-phonon excitation, the existence of a degenerate 0^+, 2^+, 4^+ triplet of states at twice the energy of the first 2^+. Experimentally, all members of the triplet are rarely observed, and their excitation energy is usually somewhat more than twice that of the first 2^+ state. In the harmonic oscillator approximation, transitions from the ground to excited states above the first are forbidden. There have been a number of recent developments in the theory of these vibrational excitations (referred to by Stelson,[22] Davydov,[23] Moore,[24]

[20] P. H. Stelson and F. K. McGowan, Phys. Rev. (to be published).

[21] *Proceedings of the International Conference on Nuclear Structure, Kingston, Canada*, edited by D. A. Bromley and E. W. Vogt (University of Toronto Press, Toronto, Canada, 1960), p. 788 and elsewhere.

[22] Reference 20; and reference 21, pp. 787–800.

[23] A. S. Davydov, reference 21, pp. 801–813.

[24] R. B. Moore and W. White, reference 21, pp. 640–643.

TABLE III. Gamma-ray transition-rate measurements for transitions ending in the ground state as determined by electron-scattering techniques compared with measurements by other techniques. The electron-scattering measurements of Helm (reference b) were made with poorly defined absolute cross sections, and the uncertainties from this source of error are not present in the other electron-scattering results. The letters "B. A." indicate transitions for which the Born-approximation analysis should be valid. The source of the discrepancy in the measurements of the 2.18-Mev transition in Li^6 is not understood at present.

Nuclide	Level (Mev)	Excited state spin-parity assignment, transition multipole	Γ_{es} (sec^{-1})	Ref	Γ_{other} (sec^{-1})	Ref	Method	Remarks
Li^6	2.18	$E2$	$\left(6.1^{+4.5}_{-2.3}\right)\times10^{11}$	a	4.5×10^{10}	d	Doppler shift	B. A.
Li^6	3.56	$M1$	$(9.4\pm0.9)\times10^{15}$	a	$\left(1.38^{+0.3}_{-0.23}\right)\times10^{16}$	e	Doppler shift	B. A.
C^{12}	4.43	$E2$	$(1.89\pm0.25)\times10^{13}$	b	2.04	f	resonance fluorescence	B. A.
C^{12}	15.1	$M1$ ($T=1$)	$\left(6.0^{+1.2}_{-0.9}\right)\times10^{16}$	a	$(8.61\pm1.5)\times10^{16}$	g	elastic γ scatter	B. A.
Mg^{24}	1.37	$E2$	$(5.18\pm1.74)\times10^{12}$	b	$(1.0\pm0.4)\times10^{12}$	h	resonance fluorescence and others	B. A.
Si^{28}	1.78	$E2$	$(1.67\pm0.56)\times10^{12}$	b	$(1.37\pm0.3)\times10^{12}$	i	Doppler shift	B. A.
Ni^{60}	1.33	$E2$	$(1.27\pm0.15)\times10^{12}$	c	$(0.90\pm0.16)\times10^{12}$	j	resonance fluorescence	
Pb^{208}	2.60	$E3$	$(3.8\pm1.0)\times10^{10}$	c	$(2.5\pm1.2)\times10^{10}$	k	direct measurement	

[a] W. C. Barber, F. Berthold, G. Fricke, and F. Gudden, Phys. Rev. **120**, 2081 (1960).
[b] R. H. Helm, Phys. Rev. **104**, 1466 (1956).
[c] Present paper.
[d] F. Däublin, F. Berthold, P. Jensen, Z. Naturforsch. **14a**, 208 (1959).
[e] L. Cohen and R. A. Tobin, Nuclear Phys. **14**, 243 (1959).
[f] V. K. Rasmussen, F. R. Metzger, and C. P. Swann, Phys. Rev. **110**, 154 (1958).
[g] From measurements referred to in F. Ajzenberg-Selove and T. Lauritsen, Nuclear Phys. **11**, 1 (1959). See also, E. Hayward and E. Fuller, Phys. Rev. **106**, 991 (1957); E. L. Garwin, *ibid.* **114**, 143 (1959).
[h] See the several references in reference 15, p. 21.
[i] S. Ofer and A. Schwartzschild, Phys. Rev. Letters **3**, 384 (1959).
[j] F. R. Metzger, Phys. Rev. **103**, 983 (1956).
[k] A. W. Sunyar (private communication).

Belyaev,[25] and Grechushina[26]), among them analysis by Davydov and Filippov[27] considering deformations having triaxial symmetry, and others treating in more detail the interaction of the valence nucleons with the nuclear surface. Other authors have considered vibrational configurations involving phonons of other than quadrupole surface deformation.[28,29] Some of these descriptions can be derived by shell-model calculations. They reproduce the energies and collective behavior of a number of $E1$ and $E3$ states.[29,30]

A nuclear shape of multipole order λ may be conveniently described by the parameters $\beta_\lambda{}^d$ and γ_λ, where $\beta_\lambda{}^d$ measures the distortion and γ_λ the degree of departure from axial symmetry. Call $\beta_{2,0}{}^d$ the value of $\beta_2{}^d$ describing the rms quadrupole distortion of the nuclear ground state.[14,31] Its value may be found from $B(E2, 2^+\rightarrow 0^+)$ for the transition from the first excited to the ground state. In general, $\beta_{2,0}{}^d$ is small for the nuclei of the type considered here. Large values of $\beta_2{}^d$ describe nuclei having large spheroidal deformations; this is characteristic of many of the rare-earth elements. Extremely small values or zero characterize the closed-shell nuclei.[32,33] These various values reflect the strength of the coupling of the nucleons in unfilled shells to the nuclear surface. Strong coupling is associated with nuclei having large spheroidal deformations and weak coupling[34] with nuclei at or near closed shells. It is significant that no collective quadrupole excitations are seen in magic nuclei: the consequence of a coupling strength insufficient to generate the necessary quadrupole deformations.

In odd-A nuclei, the intrinsic nucleonic degrees of freedom are coupled to the collective oscillations,[14] giving rise to an excited-state multiplet arrayed from the vector combinations of the intrinsic and collective angular momenta. If the coupling could be neglected, the phonon excitation spectrum would be the same as that of neighboring even-even nuclei and in the absence of changes in the intrinsic structure the transition rates would exhibit the same enhancement. Weak coupling would lift the energy degeneracy of the multiplet, but if, as in the present experiment, measurements were made with energy resolution too low to resolve the multiplet, the rule of spectroscopic stability[35] would indicate that

[25] S. T. Belyaev, reference 21, pp. 587–589.
[26] D. P. Grechushina, reference 21, pp. 614–616.
[27] A. S. Davydov and G. F. Filippov, Nuclear Phys. **8**, 237 (1958); **10**, 654 (1959).
[28] A. M. Lane and E. D. Pendlebury, Nuclear Phys. **15**, 39 (1960).
[29] G. E. Brown, J. A. Evans, and D. J. Thouless (to be published); see also, B. J. Raz, Phys. Rev. **114**, 1116 (1959), which contains references to earlier work.
[30] M. Baranger, Phys. Rev. **120**, 957 (1960).
[31] Cf. P. H. Stelson, reference 21, p. 788, which contains a number of references to experimental determinations of $\beta_{2,0}{}^d$.
[32] W. W. True, Phys. Rev. **101**, 1342 (1955); and W. W. True and K. W. Ford, *ibid.* **109**, 1685 (1958).
[33] J. C. Carter, W. T. Pinkston, and W. W. True, Phys. Rev. **120**, 504 (1960).
[34] A. de-Shalit, Phys. Rev. **113**, 547 (1959).
[35] E. U. Condon and G. H. Shortley, *The Theory of Atomic Spectra* (Cambridge University Press, New York, 1953), p. 20.

the cross sections should be essentially the same as in neighboring even-even nuclei.

A set of parameters[14] appropriate to the harmonic oscillator approximation to the nucleon surface energy of a deformation of multipole order λ consists of the phonon energy ϵ, the mass transport parameter B_λ, and the effective surface tension C_λ describing the surface oscillations of an irrotational incompressible liquid drop. The relations between these and $\beta_\lambda{}^d$ are

$$(\beta_\lambda{}^d)^2=(2\lambda+1)(\epsilon/2C_\lambda), \tag{10}$$

$$\epsilon=\hbar(C_\lambda/B_\lambda)^{\frac{1}{2}}, \tag{11}$$

$$B_\lambda=\left(\frac{3ZeR^\lambda}{4\pi}\right)^2\frac{\hbar/\epsilon}{2B(E\lambda;\lambda\rightarrow 0)}. \tag{12}$$

The values of C_λ and B_λ found from Eqs. (11) and (12) are appropriate to a uniform charge distribution of radius R. The modification that takes account of a nonuniform distribution $\rho(r)$ has been published by Tassie.[36] The result, from the derivations of Lane and Pendelbury,[28] replaces $3R^\lambda$ by $(2\lambda+1)\langle r^{2\lambda-2}\rangle/R^{\lambda-2}$. With this replacement, Eq. (12) becomes

$$B_\lambda=\left[\frac{Ze(2\lambda+1)\langle r^{2\lambda-2}\rangle}{4\pi R^{\lambda-2}}\right]^2\frac{\hbar/\epsilon}{2B(E\lambda;\lambda\rightarrow 0)}. \tag{13}$$

For comparison, the prediction for B_λ using the hydrodynamical model describing the collective motion as the irrotational flow of an incompressible liquid drop is

$$(B_\lambda)_{\rm hyd}=\frac{2\lambda+1}{\lambda}\frac{AM}{4\pi}\frac{\langle r^{2\lambda-2}\rangle}{R^{2\lambda-4}}, \tag{14}$$

where A is the nuclear mass number and M is the nucleon mass.

Following Lane and Pendlebury,[28] the quantity $\langle r^{2\lambda-2}\rangle$ was evaluated for the cases of interest for a proton density distribution of the form

$$\rho(r)=\rho_0[1+e^{(r-R)/z}], \tag{15}$$

using values of the parameters r and z from the electron-scattering determination of Crannell *et al.*[1] The calculations were made on the Stanford Computation Center Burroughs 220 digital computer.

In the analysis and interpretation of the measurements discussed in Secs. IV and V, we have calculated the values of B_λ, C_λ, and $\beta_\lambda{}^d$ for a number of the observed transitions, and compared these values with other measurements. These results are included in Table IV. In addition, the values of the reduced transition probability $B_n(\lambda\rightarrow 0)/e^2$ for a number of transitions in the even-even nuclei from states n of spin λ to the ground state have been compared with the sum rule,

$$\sum_n[B_n(\lambda\rightarrow 0)/e^2]=\langle 0|Q_{\lambda 0}{}^2|0\rangle, \tag{16}$$

which can be written

$$\sum_n[B_n(\lambda\rightarrow 0)/e^2]=(Z/4\pi)\langle r^{2\lambda}\rangle, \tag{17}$$

where $Q_{\lambda 0}$ is the electric 2^λ-pole operator, and we use the notation of Lane and Pendlebury.[28] These comparisons are shown in Table V and are similar to ones made in reference 28. The approximate nature of the sum rules is shown by the values greater than unity for the expression $B(\lambda\rightarrow 0)/e^2$ divided by the appropriate sum rule limit for a number of the transitions.

In parts B and C of this section, the conclusions drawn from the values of the sum rules and collective parameters are discussed separately for the nickel and cobalt targets (referred to as "group I") and the lead and bismuth ("group II"). The energy levels in the nuclei of groups I and II are shown in Figs. 13 through

TABLE IV. Vibrational parameters for the levels in the even-even nuclei in the present experiment: $B(E\lambda)$ is the reduced transition probability; B_λ and C_λ are the mass transport and the effective surface-tension parameters of the harmonic-oscillator approximation to the nuclear surface energy; $(B_\lambda)_{\rm hyd}$ is the value appropriate to a hydrodynamic model; $\beta_\lambda{}^d$ is the distortion parameter of a nuclear shape of multipole order λ; and R is the nuclear radius ($R=R_0A^{\frac{1}{3}}$ for $R=1.20$ f).

Multipole	Nuclide	ϵ (Mev)	$B(E\lambda)/B(\lambda)_{\rm sp}$	$B_\lambda/\hbar^2$ (Mev)$^{-1}$	$(B_\lambda)_{\rm hyd}$	$B_\lambda/(B_\lambda)_{\rm hyd}$	C_λ (Mev)	$\beta_\lambda{}^dR$ (f/Mev)
$E2$	Ni^{58}	1.45	14.3 ±1.9	69.5± 9	4.16	16.7 ±2.2	145± 19	0.745 ±0.097
	Ni^{58}	3.2	4.45±1.6	106 ± 38	4.16	25.6 ±9.2	1070±390	0.407 ±0.15
	Ni^{60}	1.33	17.1 ±2.1	65.2± 7.8	3.96	16.45±2.0	116± 14	0.792 ±0.095
$E3$	Ni^{58}	4.50	13.2 ±1.8	103 ± 14	4.45	23.2 ±3.2	2090±290	0.401 ±0.056
	Ni^{60a}	4.05	15.9 ±2.5	88.5± 14	4.61	19.3 ±3.1	1450±230	0.464 ±0.074
	Ni^{60b}	5.1	7.8 ±1.8	144 ± 34	4.61	31.2 ±7.4	3700±875	0.324 ±0.077
	Pb^{208}	2.60	30.8 ±11	280 ±105	23.8	11.7 ±4.2	1890±700	0.495 ±0.18
$E4$	Ni^{58}	2.50	2.2 ±0.66	6140±1800	6.96	870±260	(3.84±1.2)×10⁴	0.0791±0.024
	Ni^{58}	3.51	2.5 ±0.57	1196± 270	6.96	1720±400	(1.46±0.33)×10⁴	0.15 ±0.035
	Ni^{60}	2.50	3.62±0.69	3400± 650	6.84	494± 94	(2.12±0.40)×10⁴	0.104 ±0.02
	Ni^{60}	5.1	4.95±0.74	1230± 185	6.84	180±270	(3.20±0.48)×10⁴	0.125 ±0.019
	Pb^{208}	4.30	36.6 ±12	495± 160	24.7	20.0±6.5	(9.34±3.1)×10³	0.327 ±0.11

[a] See McDaniels *et al.*, reference 37.
[b] Preferred multipole is $E4$.

[36] L. J. Tassie, Australian J. Phys. **9**, 407 (1956).

TABLE V. Comparison of $B(\lambda \to 0)$, the reduced transition probability for multipole order λ, for a number of transitions in even-even nuclei, with the sum-rule limits as determined from Eq. (17). Here, Z is an antisymmetrization factor whose value is between 0.5 and 1.0, as used by Lane and Pendlebury (reference 28). The approximate nature of these sum rules is indicated by the values greater than unity found for the $E2$ transitions. No theory or interpretation appropriate to a sum-rule analysis of the $E4$ transitions observed in the present experiment is available, and comparisons have accordingly been omitted from the analysis.

Multipole	Nuclide	Sum-rule limit $\left[\frac{B(\lambda \to 0)}{e^2}\right]_m$ / sum $\left[\frac{B(E2, \lambda \to 0)}{e^2}\right]_m$			Fractional error	Remarks
$E2$	Ni^{58}	6.56×10^2 f^4	$1.51/Z$	9.9×10^2 f^4	0.13	1.45-Mev level only
			$1.98/Z$	13.0×10^2 f^4	~0.15	Including 3.2-Mev level
	Ni^{60}	6.76×10^2 f^4	$1.84/Z$	1.25×10^3 f^4	0.12	1.33-Mev level
	Pb^{208}	2.30×10^3 f^4	...	...	...	No $E2$ transitions observed
$E3$	Ni^{58}	1.76×10^4 f^6	$0.154/Z$	2.7×10^3 f^6	0.14	4.50-Mev level
	Ni^{60}	1.83×10^4 f^6	$0.190/Z$	3.5×10^3 f^6	0.16	4.05-Mev level
	Pb^{208}	3.0×10^5 f^6	$0.27/Z$	8.1×10^4 f^6	0.37	2.6-Mev level

17. Also shown are many levels, known from other work, which the electron scattering process does not strongly excite.

B. Co^{59}, Ni^{58}, Ni^{60}

A variety of evidence has established the spins and parities of the first excited states of Ni^{58} and Ni^{60} as 2^+. No exception is known to the rule that the ground-state spin and parity of even-even nuclei is 0^+, thus defining the gamma transition from the first excited state to the ground state as pure $E2$ for these nickel isotopes. The systematics of these and analogous transitions in other nuclei has led to the suggestion that the first excited state represents the one-phonon excitation of a vibrational collective quadrupole deformation of the nuclear surface. In these and nuclei of similar mass, 2^+ and 4^+ higher excited states are usually identified. The 0^+ member of the two-phonon triplet (not predicted by the theory of Davydov and Filippov[27]) is usually not seen.

The measurements of these transition form factors in the nickels agree well with the $E2$ assignment. The values of G are much greater than unity, as expected from the enhancement predicted by the collective description of the excited state, and the value for Ni^{60} agrees with the value found from a resonance fluorescence measurement of the gamma lifetime (see Table III). In Co^{59}, electron scattering induces a transition strikingly similar in energy, multipole assignment, and value of β_2 (defined in Sec. IV); a transition which also has a large γ-ray transition rate enhancement. In this nucleus, the ground-state spin and parity are $\frac{7}{2}^-$, and the measured transition energy (1.30 ± 0.1 Mev) and peak width of the scattered electrons that have induced the transition suggest a transition to the known $\frac{3}{2}^-$ at 1.29 Mev. The multiplet expected on the vibrational interpretation of the excited-state configuration would have five components with spins ranging from $\frac{3}{2}$ to 11/2 and negative parity. We saw no appreciable broadening of the recoil electron line, which would indicate that the energy degeneracy of the multiplet is not lifted by as much as 300–400 kev. Two arguments suggest that the degeneracy is not lifted by an amount large compared to the experimental resolution. The first is that one would expect to distinguish the several members of the multiplet in inelastic electron scattering, and no other low-lying $E2$ transitions were seen in the present experiment. The second is that such a splitting would indicate a valence nucleon-surface coupling term far stronger than that currently accepted for this mass region. We are puzzled why the other levels of this multiplet in Co^{59} have not been identified in higher-resolution nuclear reaction or decay scheme studies. Electron excitation fails to excite the 1.10-Mev $\frac{5}{2}^-$ first excited state, and the conclusion is that this transition fails to have a strong $E2$ enhancement and thus is not to be identified as one of the collective multiplet. If one assumes the transition to be to the known $\frac{3}{2}^-$ level, as in Fig. 14 and in Table II, the resulting value of G is much higher than the comparable values for the nickels. This reflects only statistical factors in the expressions for Γ_m and Γ_{sp}. If one assumes the transition to be to all members of the unresolved multiplet and averages over intensities to all the components, then the average value of $G=B(E2)_{ph}/B(E2)_{sp}$ is about 11, where $B(E2)_{ph}$ is the value appropriate to the phonon excitation and is defined in Eq. (V. 32) of Alder *et al.*[14]; $B(E2)_{ph}$ is equivalent to the $B(E2, 2^+ \to 0^+)$ for the nickel isotopes. This similarity of the values of G reflects the similarity of the values of β_2 for this transition in group I. These similarities and the near identity of the transition energies lead us to conclude that the collective quadrupole vibrational state is being excited in all three nuclei, and that the only discernible effects of differences in the valence nucleon configurations among the three are in slight changes in ϵ and β_2.

The known $E4$, $0^+ \to 4^+$ transition to the 2.50-Mev level in Ni^{60} is excited by electron scattering, and the measured form factor may be fitted unambiguously with an $E4$ assignment. In addition to this $E4$ transition, analogous ones are excited in the other two nuclei of group I. They all have nearly identical energies (2.70 Mev in Co^{59}, and 2.50 Mev for both nickels), and comparable values of β_4 (see Table I). The values of G observed are not substantially greater than unity. In

Co^{59}, the peak was poorly resolved at many angles, and the measured form factor disagreed with the prediction at the two lowest values of θ. In view of the errors associated with these measurements, the disagreements are not considered serious. The data establish the similarity of the transitions at the several points at which the peak is well resolved. The very small values of G compared with the other collective transitions are qualitatively understood on the basis of the two-phonon interpretation of the excited-state configuration.

The measurement of the gamma transition rate for the 2.50-Mev $E4$ transition in Ni^{60} was combined with the data of Morinaga and Takahashi[19] on the ratio of the intensity of this 2.50-Mev ray to the 1.17-Mev ray leading to the 2^+ excited state at 1.33 Mev, to yield a value for the partial transition rate for the 1.17-Mev $E2$ transition, and hence of the rate enhancement G. The errors attached to the measurement of this ratio are not known. The value of G is 0.85, which is a low value not understood on the basis of the vibrational model.

$E3$ transitions having similar energies around 4 Mev were observed in each of the nuclei of group I. The form factors had the same q dependence within the errors of measurement, and the values of β_λ were nearly the same for the nickels and about a factor of two lower for Co^{59}. The values of G indicate strong enhancement of the gamma transition rate. The $E3$ assignments for these transitions in group I are unambiguous, and for Ni^{58} and

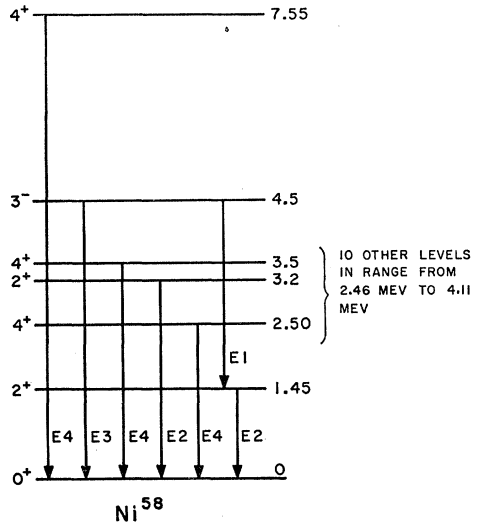

FIG. 13. In this and the following four figures are shown portions of the energy-level structures of the nuclei investigated in the present experiment. The information is, for the most part, taken from reference 15. The γ-ray transitions shown are those whose decay rates were determined directly in the present experiment or inferred from a knowledge of the γ-ray branching ratios in de-excitation of the nucleus. The spin and parity of each level are shown at the left, where known, and the energy of the excited states in Mev on the right. The best assignments of the transition multipolarities are indicated. This figure shows the energy-level structure of Ni^{58}.

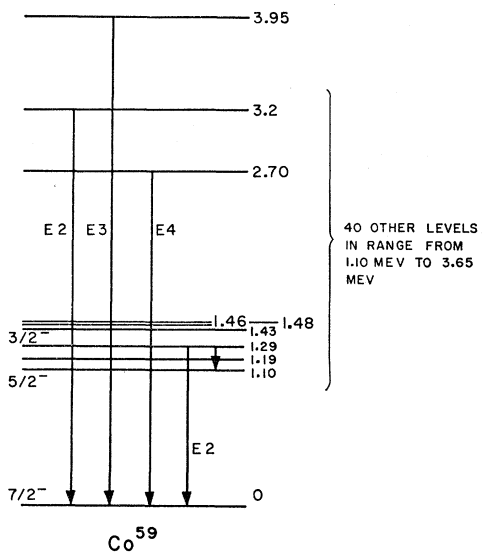

FIG. 14. Energy-level diagram for Co^{59}. A large number of the energy levels are omitted (see reference 16). We have identified the 1.30-Mev transition induced by inelastic electron scattering with the 1.29-Mev transition known from other studies (see references 15 and 16). It is expected, from other considerations discussed in the text, that each observed electron-induced transition may excite a number of levels spaced less than about 200 kev apart. This possibility adds some uncertainty to the level scheme and to the measurements of the gamma transition rate for the 0.19-Mev ray from the 1.29-Mev level. See caption for Fig. 13.

Ni^{60} they agree with those made by Crut *et al.*[37] on the basis of angular correlation measurements and by McDaniels *et al.*[38] using inelastic α-particle scattering. The multiplet expected in Co^{59} is unresolved. These transitions are among the class of "anomalous" transitions first seen by Cohen and co-workers[39] in inelastic proton scattering. These have been seen over wide regions of the periodic table, and, unlike the collective $E2$ transition, they vary only slightly in properties from one region to another. The $E3$ transitions seen in group I are of the same class as the two seen in group II.

These octupole transitions are interpreted as the lowest collective octupole vibrational mode of nuclei not having large ground-state deformations. Alternative single-particle descriptions have also been proposed,[40] but the interpretation as collective excitation is more satisfactory. Lane and Pendlebury[28] have recently studied this interpretation theoretically and concluded that the octupole states are not well described as single-particle states. More sophisticated shell-model predictions using a detailed treatment of the particle-hole interaction in nuclear matter[29] and a complete shell-model analysis[33] for Pb^{208} bear out this conclusion. The

[37] M. Crut, D. R. Sweetman, and N. S. Wall, Nuclear Phys. **17**, 655 (1960).
[38] D. K. McDaniels, J. S. Blair, S. W. Chen, and G. W. Farwell, Nuclear Phys. **17**, 614 (1960).
[39] Cf. B. L. Cohen and A. G. Rubin, Phys. Rev. **111**, 1568 (1958), and earlier papers referred to there.
[40] C. D. Goodman, Phys. Rev. Letters **3**, 230 (1959).

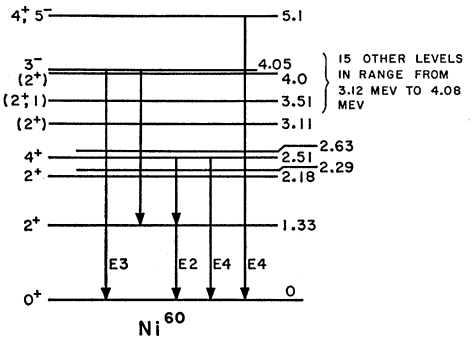

FIG. 15. Energy-level diagram for Ni^{60}. (See caption for Fig. 13.) A number of levels have been omitted from the diagram (see reference 16).

similarities of the measured form factors and energies for these transitions in group I and the substantial enhancements observed strongly support the conclusion that these are collective states and that their gross properties are independent of the valence nucleon configuration. As in the $E2$ and $E4$ transitions, the predicted multiplet is unresolved in Co^{59}, indicating that the particle-surface coupling is relatively weak.

In addition to the families of transitions seen in group I, there was a 3.5-Mev transition seen in Ni^{58} which could be fitted by an $E4$ assignment. The value of G is about 2.5. $E3$ and $E5$ assignments are probably not excluded by the data, although the fits are very much poorer. A 5.1-Mev transition in Ni^{60} is fitted by an $E4$ assignment. It is only slightly enhanced; assignments of $E3$ or $E5$ (see Table II) predict somewhat greater enhancement. A strong $E4$ transition is seen in Ni^{58} at 7.55 Mev; $G=11.6$ for this transition. There was evidence for similar transitions in Ni^{60} and Co^{59}, but they were too poorly resolved to be clearly distinguished.

The values of the deformation parameter $\beta_\lambda{}^d$ times the nuclear radius, of $B_\lambda/(B_\lambda)_{\text{hyd}}$, and of C_λ are given for the nickel isotopes and Pb^{208} in Table IV. It can be seen that the mass parameters B_λ, for $\lambda<4$, are on the average somewhat more than an order of magnitude greater than the hydrodynamic or irrotational values. These enhancements of B_λ and the magnitudes of the surface tension parameter C_λ reflect the enhancements of the γ-ray transition rates that were calculated from the measured form factors. The B_λ, and especially B_2, are very sensitive to the strengths of the valence nucleon-surface interactions, and the observed values are in qualitative agreement with the predictions of the collective model. Values of these parameters have been reported by a number of authors.[31,32,41] The behavior of the quadrupole parameters throughout the periodic table has been interpreted by Marumori *et al.*,[42] assuming vibrational collective excitations, and Pendlebury and Lane[28] give an analogous discussion for the octupole parameters. The very large values of β^4 and the large fluctuations in their values normalized to predictions of the hydrodynamic model are not understood, no theoretical interpretation being available.

C. Pb^{208}, Bi^{209}

A large number of shell-model calculations have been made in attempts to describe the level structure of the nuclides near Pb^{208} in terms of data on the single-particle levels in the particularly rigid structure of this doubly-magic nucleus.[32,33,43] The rigidity of this structure is testified to by the absence of collective quadrupole states (none is known in Pb^{208}), the high energy of the first excited state (the highest of any nucleus of $A>40$), the slowness of electric-quadrupole transitions in nuclei whose A is close to 208, and the measurement of the core deformation by the odd proton in Bi^{209} through measurement of its static quadrupole moment.[44] The shell-model calculations have been successful in predicting the level positions and spins of a large number of levels for other Pb isotopes. In Pb^{208}, analogous calculations are more difficult than for neighboring nuclei because, in a shell-model description, all excited states must involve the breaking of the core configuration and thus require a detailed knowledge of two-nucleon interactions in the nucleus.

A number of authors have suggested single-particle descriptions for the 2.60-Mev first excited 3^- state in Pb^{208}, although there are strong theoretical objections to these. Carter, Pinkston, and True's shell-model calculation[33] shows that there is no single-particle configuration that explains the excited state energy. The complexity of the decay scheme[15] of Pb^{208} makes a reliable γ-ray transition-rate measurement for this transition very difficult, and hence also the determination of the collective enhancement. Inelastic electron scattering excites this level strongly, and the measurements show (see Table II and Fig. 10) a gamma transition rate enhancement of 30.8. This value is nearly identical to the recent prediction of this quantity by Baranger.[30] A transition of the same energy in Bi^{209} was observed in the present experiment, having a form factor the same within experimental error. The inelastic form factors of the transition in both nuclei fit $E3$ predictions. As before, we assume we are observing, in Bi^{209}, the unresolved multiplet containing several states of spins from $\frac{3}{2}$ to 15/2. The transition rates in Table II are evaluated for the two states with spin $I_e=\frac{3}{2}$ and $I_e=15/2$. The value of $B(E3)_{\text{ph}}$ is, from the value of β_3, nearly the same as that for the excitation in Pb^{208}; the great similarity between these transitions in the two isotopes, coupled

[41] P. H. Stelson and F. K. McGowan, Phys. Rev. **110**, 489 (1958).

[42] T. Marumori, S. Suekane, and A. Yamamoto, Progr. Theoret. Phys. (Kyoto) **16**, 320 (1956).

[43] I. Bergström and G. Andersson, Arkiv Fysik **12**, 415 (1957), have reviewed a number of the shell-model calculations for $A\simeq 208$.

[44] The single-particle levels for nuclei in the region about Pb^{208} are given by A. E. S. Green, Phys. Rev. **104**, 1620 (1956).

with the enhancement of the gamma transition rates, demonstrates a predominantly collective configuration for both levels. If the 2.3-Mev level in Pb^{208} would be $(d_{3/2})^{-1}(h_{9/2})$ configuration,[44] the analogous state in Bi^{209} would be $(d_{3/2})^{-1}(h_{9/2})^2$, and the pairing interaction would be expected to lower the energy of the state by far more than 300 kev, an amount incompatible with the present measurements. There was no evidence for the electron excitation of the first two levels in Bi^{209}, levels which this result suggests will have predominantly single-particle configurations.

In addition to the pair of 2.60-Mev electric octupole transitions, we observed a second pair of transitions, each of 4.30-Mev energy, one transition in each nucleus, having, within the experimental error, the same transition form factors. The predictions for $E3$ fail, contrary to an earlier report,[17] and the form factors are fitted best by an $E4$ assumption. The $E4$ fit is not as satisfactory as for the $E4$ transition in Group I, but is within the range of agreement expected from the theory employed and the errors introduced during the data processing. An $E5$ assignment is probably not excluded, but it appears quite unlikely when compared with other fits discussed earlier. With any of these assignments, the γ-ray transition rates are strongly enhanced; for the $E4$ assumption, the enhancement in Pb^{208} is 36.6. Our failure to observe transitions to a large number of the known levels in both Pb and Bi in the range of nuclear excitations from 0.90–4 Mev (see Figs. 16 and 17), and the large enhancements of the identical 4.30-Mev transitions, suggest that we are observing a collective excitation whose detailed configuration is unknown. It is apparent from the values of G that the configuration is quite different from that of the 4^+ states in Group I nuclei. It appears possible that this common collective configuration may be the one-phonon 4^+ vibrational state distinguished by its value of G from a two (2^+)-phonon 4^+ excitation.

As in the collective states in cobalt and nickel, one is led to the conclusion that the important contributions to the structures of the 2.60- and 4.30-Mev states in the odd-A isotope Bi^{209} are the same as the collective configuration in the even-A isotope Pb^{208}. The excited configurations in Bi^{209} then consist of multiplets with seven and nine components, respectively. The present measurements are consistent with the multiplets' being energy degenerate or nearly so. The situation is analogous to the investigations of Cohen *et al.*[39] using inelastic proton scattering to study the electric octupole transitions. In those studies, using low energy resolution, the splitting of the collective configuration by different single-particle states was undetectable, whereas at higher resolution the structure could be well resolved. The point is discussed by Lane and Pendelbury.[28] In Table II, the values of Γ_m and G are computed for the two excited states with the highest and lowest spins relevant to each multiplet. The differences in the values of Γ_m and G from those observed in Pb^{208} arise entirely from statistical factors. The values of β_λ for the $E3$ and separately for the $E4$ transitions are the same within the errors of measurement.

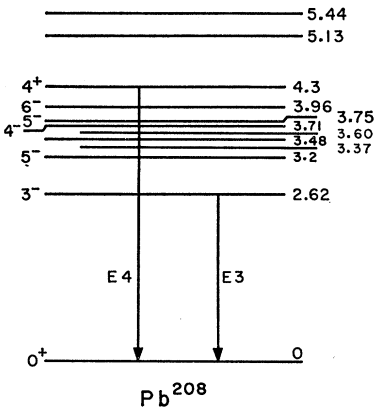

FIG. 16. Energy-level diagram for Pb^{208} showing the known excited states below 5.5 Mev. (See caption for Fig. 13.)

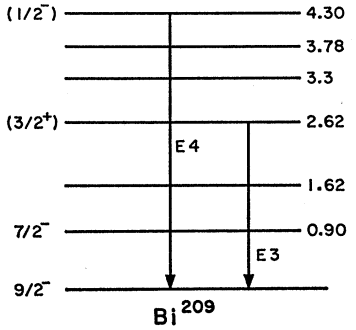

FIG. 17. Energy-level diagram for Bi^{209} showing the known excited states below 4.5 Mev. The spin assignments in brackets are the lowest values compatible with the assigned transition multipolarities. It is expected that the electron excitation process may excite groups of states with an energy spacing less than about 200 kev. The consequences of excitation of groups of states, unresolved in the present experiment, are not incorporated in the diagram but are described in the text.

VII. CONCLUSIONS

In spite of the shortcomings of the Born-approximation analysis of the inelastic scattering, it appears to yield better estimates of the γ-ray transition rates than there is any reason to expect, especially in the high-Z elements. The rates determined in this way are rarely in error by a factor of two when absolute cross-section measurements are available. Inasmuch as the γ-ray enhancements can vary by factors greater than 100, depending on the characters of the transitions, it is apparent that the measurements can prove useful in interpreting these characters in spite of the uncertainties introduced by the analysis.

The deficiencies in the analysis of the inelastic-scattering results have one important consequence: to deny us access to the information contained in the measured form factors concerning the spatial distribution of the transition matrix elements, and hence of the spatial structure of the excited-state wave functions. Phase-shift analysis of elastic scattering allows precise deter-

minations of static nuclear charge distributions, for the high momentum transfers necessary to study the very short distance structure of the distributions are easily obtained. Equivalent information is contained in the inelastic form factors reported here. In the present experiment we extract only the most rudimentary information about the excited-state wave functions, namely, that the scattering to a level of known properties can be predicted, in the region away from the Born zeros, assuming that the important contributions to the transition matrix elements depending on these wave functions arise from the region near the nuclear surface.

One of the techniques employed in the present measurement was to investigate transitions in groups of nearly identical nuclei. We have observed a number of different sets of similar transitions in these groups, each set having form factors that were strikingly similar even in the region of the Born zeros. These data establish the similarity of the nuclear excited-state configurations in these groups of nuclei in a manner independent of analysis. These similarities, coupled with the large γ-ray enhancements observed, suggest that these configurations are in large part collective, and support in a number of cases the conclusions of other workers.

The values of the collective vibrational parameters, being based on these observed enhancements, serve to indicate in an equivalent way that these states are of a collective nature.

One of the questions raised by the present results is: Why do we fail to see so many of the known levels in the region of excitation under examination? In Co^{59} there are over 40 known levels, of which only two are excited with large probability. In Pb^{208} only two out of about ten levels under 5.5-Mev excitation are seen. The situation is the same in the other nuclides. By no means are all the missing levels the magnetic transitions that the Born approximation suggests would not be strongly excited. Gamma-ray enhancement measurements do not appear to be as good a guide in answering this question as might have been expected, for a few transitions were observed which in fact were little faster than single-particle speed. The results appear to indicate that the electron-scattering process selects the class of collective excited-state configurations.

We summarize here briefly the results discussed in the earlier sections.

(1) In Ni^{58}, Ni^{60}, and Co^{59}, we observed the known fast $E2$ transitions which in the even-even isotopes lead to the first excited state. The enhancement known for the Ni^{60} transition was confirmed, and similar enhancements were found for the other two. The form factors for all three were nearly identical for all momentum transfers investigated, including those in the region where the measurements disagree greatly with the Born-approximation predictions.

(2) In the same group of nuclei and in Pb^{208} and Bi^{209}, the "anomalous" $E3$ transitions were seen. In all cases, the gamma transition rates show substantial enhancement compared to single-particle predictions. In the odd-A elements there appears to be no evidence for lifting of the energy degeneracy of the multiplet formed from the angular momentum of the excitation and the spin of the ground-state configuration. The energy resolution used was, however, not sufficient to resolve splittings less than about 0.4 Mev. The data strongly support the conclusion that the states are predominantly collective.

(3) $E4$ transitions in Ni^{58}, Ni^{60}, and Co^{59} were observed which had similar form factors. In Ni^{60}, the transition was to the known 4^+ state at 2.50 Mev. In all cases, the gamma transition rates were close to the single-particle predictions. Other evidence allows an interpretation of the levels as being predominantly collective.

(4) A pair of transitions in Pb^{208} and Bi^{209} have identical energies (4.30 Mev) and form factors. They are identified as enhanced $E4$ transitions, and are probably the second collective excited states in these nuclei, the first 16-pole excitations rather than double $E2$ phonon excitations.

(5) No electric-quadrupole transitions were seen in either Pb^{208} or Bi^{209}.

(6) Three $E4$ transitions were seen in the nickel isotopes, a 5.1-Mev transition in Ni^{60} and 3.5-Mev and 7.55-Mev transitions in Ni^{58}; of the three, only the 7.55-Mev transition is appreciably enhanced.

(7) A large number of known states in the nuclei investigated here were excited so weakly as to be unobservable. This result can be understood qualitatively for some of the states, but for the majority it cannot. It would appear that the electron-scattering process selectively excites certain types of excitations. The evidence indicates these may be collective, but the present theory of the inelastic-scattering process is inadequate to demonstrate this conclusion unambiguously.

ACKNOWLEDGMENTS

We wish to thank a number of people for their help with the experimental equipment and the numerical analysis of the data. L. Buss constructed and L. Doster helped maintain the electronic equipment. Professor R. Mozley, R. G. Gilbert, and the staff of the Stanford accelerator operated and maintained the machine during the data taking. Professor D. Teichoew very kindly made an IBM-610 digital computer available, and R. Braden, R. Gordon, and A. Collins helped with the programming of the Stanford Computation Center's Burroughs 220 computer. We are grateful to Professor L. I. Schiff, Professor J. D. Walecka, and Professor W. C. Barber, of Stanford, and Professor Gerald E. Brown and Professor Amos de-Shalit for a number of illuminating discussions. We thank Professor R. Hofstadter for his support of this work.